Proceedings of the 17th World Congress
The International Federation of Automatic Control
Seoul, Korea, July 6-11, 2008

Disturbance Suppression beyond Nyquist Frequency in Hard Disk Drives

Takenori Atsumi *

* *Central Research Laboratory, Research & Development Group, Hitachi, Ltd., 1 Kirihara, Fujisawa, Kanagawa 252–8588, Japan (Tel: +81-466-98-4166; e-mail: takenori.atsumi.ta@hitachi.com).*

Abstract: In conventional hard disk drives, a control system compensates for vibration in which the frequency is higher than the Nyquist frequency by using a multi-rate filter that decreases the gain above the Nyquist frequency. However, such a control system can only avoid instability and cannot suppress disturbances above the Nyquist frequency. In response to this problem, a control system design method that suppresses disturbances beyond the Nyquist frequency is proposed. This method uses frequency responses of a controlled object and a digital controller to calculate the gain of the sensitivity function in a sampled-data system without requiring complex calculations involving matrices, and realizes a stable resonant filter that decreases the gain of the sensitivity function above the Nyquist frequency. When the method was applied to the head-positioning system of a hard disk drive, the experimental results showed that the control system suppressed disturbances above the Nyquist frequency.

Keywords: Mechatronic systems; Tracking; Disturbance rejection; Vibration and modal analysis; Design methodologies.

1. INTRODUCTION

The head-positioning accuracy of hard disk drives must be improved to meet the increasing demand for larger storage capacity [Lyman et al. (2003)]. In the head-positioning system of a hard disk drive, vibrations of the mechanical system impair positioning accuracy. Therefore, it is important to compensate for the vibrations in the head-positioning system to improve positioning accuracy [Atsumi et al. (2003, 2005)].

The head-positioning system of a hard disk drive is implemented in a sampled-data control system that has a sampler and a hold. The head-positioning system also has mechanical vibrations whose frequencies exceed the Nyquist frequency of the control system. As such, the head-positioning control system needs to compensate for mechanical vibrations above the Nyquist frequency.

The control system in conventional hard disk drives compensates for these vibrations by using a multi-rate filter that decreases the gain above the Nyquist frequency [Weaver et al. (1995)]. However, such control systems can only avoid the instability caused by mechanical resonances; they cannot actually suppress the vibrations. Many studies have been done on control systems that improve the control performance on the basis of sampled-data control theories and multi-rate control techniques [Hirata et al. (1999); Gu et al. (2000); Semba (2001); Hara (2006)]. However, these studies don't focus on how to suppress the vibrations with frequencies higher than the Nyquist frequency.

In response to the above-mentioned problems, a control system that suppresses disturbances beyond the Nyquist frequency is proposed. The design method for the control system uses frequency responses of a controlled object and a digital controller for calculations of the gain of the sensitivity function in a sampled-data system without requiring complex calculations involving matrices. When the method was applied to the head-positioning system of a hard disk drive, the experimental results indicated that the control system suppressed the vibrations caused by the disturbances beyond the Nyquist frequency.

2. HEAD-POSITIONING SYSTEM OF HARD DISK DRIVES

A hard disk drive consists of a voice coil motor (VCM), several magnetic heads, several disks, and a spindle motor. The head-positioning control system in hard disk drives is illustrated in Fig. 1. In the head-positioning system, the control variable is the head-position signal, which is embedded in disks and is read by magnetic heads. This means the head-position signal is only available as a discrete-time signal. The control input is the voltage supplied to a power amplifier that drives the VCM and magnetic heads, which is calculated by a digital signal processor at certain intervals. Therefore, a head-positioning control system can be thought of as a sampled-data control system that has a sampler and a hold.

A block diagram of the sampled-data control system with a multi-rate digital filter is shown in Fig. 2. Here, $\mathcal{S}$ is the sampler, $C[z]$ is the single-rate digital controller, $I_p[z]$ is the interpolator, $F_m[z]$ is the multi-rate digital filter, $\mathcal{H}_m(s)$ is the multi-rate hold, $P_c(s)$ is the continuous-time plant, r is the reference signal, u_d is the output signal from $C[z]$, u_c is the output signal from $\mathcal{H}_m(s)$, d_c is the disturbance signal in continuous time, y_{c0} is the

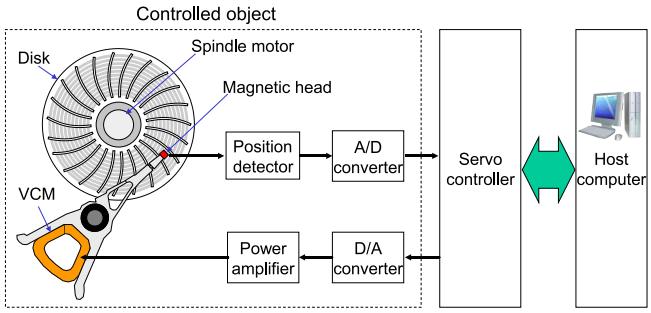

Fig. 1. Head-positioning system in hard disk drive

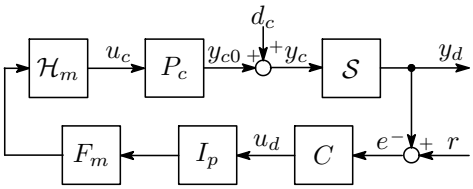

Fig. 2. Block diagram of sampled-data control system

output signal from $P_c(s)$, y_c is the head-position signal in continuous time, and y_d is the head-position signal in discrete time. In this study, the multi-rate number is m, the sampling time is T_s [s], and the sampling frequency is $\omega_s = 2\pi/T_s$ [rad/s].

The timing used in reading or writing user data in hard disk drives corresponds to intersampling in a sampled-data control system. In other words, the essential purpose of a head-positioning system is to control the maximum displacement of the control variable including intersampling behaviors. Therefore, the control system should be designed as a sampled-data system so that the controller compensates for the intersampling vibrations.

The head-positioning system has two control modes; one is "seek control," which moves the head onto the target track, and the other is "following control," which maintains the head position on the target track. In the seek control, the main target of the control system is the transient characteristics of the head position, but in the following control, the main target is the steady-state characteristics. The purpose of this study is to develop a following control system, so from here on, the steady-state characteristic of the head position is focused.

3. ANALYSIS OF SAMPLED-DATA CONTROL SYSTEM USING FREQUENCY RESPONSE

To avoid complex calculations involving matrices, the proposed method uses frequency responses to analyze the sampled-data control system. The method handles intersampling vibrations and the characteristics of disturbance rejections in a sampled-data system by using frequency responses.

The relationship between a continuous-time signal and discrete-time signal is defined in this paper. For illustration purposes, the sinusoidal wave $x_0(t)$ is defined as

$$x_0(t) = e^{j\omega_0 t}. \tag{1}$$

The discrete-time signal $x_d[n]$, which corresponds to the signal after sampling of $x_0(t)$ with the sampling time T_s, can be given as

$$x_d[n] = x_0(nT_s) = e^{j\omega_0 T_s n}. \tag{2}$$

The continuous-time signal $x_c(t)$, which is created from $x_d[n]$, can be given as

$$x_c(t) = \sum_{l=-\infty}^{\infty} \delta(t - lT_s)e^{j\omega_0 t} = \frac{1}{T_s}\sum_{l=-\infty}^{\infty} e^{j(\omega_0+\omega_s l)t}, \tag{3}$$

where δ is a Dirac delta function. Equations (2) and (3) indicate that the discrete-time signal caused by a single complex sinusoid can be given by a single frequency, and the continuous-time signal caused by the discrete-time signal consists of several frequencies.

3.1 Analysis of sensitivity function

In some papers, the gain-frequency response of the sensitivity function in the sampled-data system is defined by using the worst-case H_∞ norm of systems or the upper/lower bound [Hara et al. (1995); Yamamoto et al. (1996)]. However, obviously, a head-positioning system has to control the maximum displacement of the control variable, and the maximum displacement has no bound in the steady-state characteristics. Therefore, the infinity norms of signals are used for defining the gain of the sensitivity function for head-positioning control in hard disk drives. In this paper, a gain-frequency response of the sensitivity function in a sampled-data control system $|S_{sd}|$ at ω_0 is given by the following equation using d_c and y_c in Fig. 2:

$$|S_{sd}(j\omega_0)| = \frac{||y_c(t)||_\infty}{||d_c(t,\omega_0)||_\infty} = \sup_t |y_c(t)|, \tag{4}$$

where $d_c(t,\omega_0)$ is a single complex sinusoid,

$$d_c(t,\omega_0) = e^{j\omega_0 t}. \tag{5}$$

The transfer characteristics from u_d to y_d at ω_0, which is a controlled object in a discrete-time system, is given as $P_d(j\omega_0)$,

$$P_d(j\omega_0) = \frac{1}{T_s}\sum_{k=-\infty}^{\infty} W(j\omega_0 + j\omega_s k)P_c(j\omega_0 + j\omega_s k), \tag{6}$$

where

$$W(j\omega) = I_p[e^{j\omega T_s/m}]F_m[e^{j\omega T_s/m}]\mathcal{H}_m(j\omega). \tag{7}$$

In a steady state with $d_c(t,\omega_0) = e^{j\omega_0 t}$, u_d can be given by the following equation:

$$u_d[n] = \frac{-C[e^{j\omega_0 T_s}]}{1 + P_d(j\omega_0)C[e^{j\omega_0 T_s}]}e^{j\omega_0 T_s n}. \tag{8}$$

Here, $u_c(t)$ and $y_{c0}(t)$ consist of several frequencies and are given by follows:

$$u_c(t) = \frac{-C[e^{j\omega_0 T_s}]}{1 + P_d(j\omega_0)C[e^{j\omega_0 T_s}]}\frac{1}{T_s} \times \sum_{l=-\infty}^{\infty} W(j\omega_0 + j\omega_s l)e^{j(\omega_0+\omega_s l)t}. \tag{9}$$

$$y_{c0}(t) = \frac{-C[e^{j\omega_0 T_s}]}{1 + P_d(j\omega_0)C[e^{j\omega_0 T_s}]}\frac{1}{T_s} \times \sum_{l=-\infty}^{\infty} W(j\omega_0 + j\omega_s l)P_c(j\omega_0 + j\omega_s l)e^{j(\omega_0+\omega_s l)t}. \quad (10)$$

Therefore, $y_c(t)$ also consists of several frequencies and is given by

$$\begin{aligned} y_c(t) &= y_{c0}(t) + d_c(t, \omega_0) \\ &= \Gamma(\omega_0)e^{j\omega_0 t} + \sum_{l=-\infty,\neq 0}^{\infty} \Lambda(\omega_0, l)e^{j(\omega_0+\omega_s l)t}, \end{aligned} \quad (11)$$

where

$$\Gamma(\omega) = 1 - \frac{1}{T_s}\frac{C[e^{j\omega T_s}]W(j\omega)P_c(j\omega)}{1 + P_d(j\omega)C[e^{j\omega T_s}]}, \quad (12)$$

and

$$\Lambda(\omega, l) = -\frac{1}{T_s}\frac{C[e^{j\omega T_s}]W(j\omega + j\omega_s l)P_c(j\omega + j\omega_s l)}{1 + P_d(j\omega)C[e^{j\omega T_s}]}. \quad (13)$$

Finally, $|S_{sd}(j\omega_0)|$ can be given by

$$|S_{sd}(j\omega_0)| = \sup_t |y_c(t)| = |\Gamma(\omega_0)| + \sum_{l=-\infty,\neq 0}^{\infty} |\Lambda(\omega_0, l)|. \quad (14)$$

3.2 Disturbance suppression in sampled-data system

To suppress vibration in which the frequency is ω_0, the control system should have a certain level of $|WP_c|$ at ω_0 so that $|\Gamma(\omega_0)|$ becomes small and a small amount of $|WP_c|$ at the aliasing frequencies so that $\sum_{l=-\infty,\neq 0}^{\infty} |\Lambda(\omega_0, l)|$ becomes small. On the other hand, $y_d[n]$ can be given by the following equation:

$$\begin{aligned} y_d[n] &= y_c(nT_s) \\ &= \Gamma(\omega_0)e^{j\omega_0 T_s n} + \sum_{l=-\infty,\neq 0}^{\infty} \Lambda(\omega_0, l)e^{j(\omega_0 T_s + 2\pi)n} \\ &= \left(\Gamma(\omega_0) + \sum_{l=-\infty,\neq 0}^{\infty} \Lambda(\omega_0, l)\right) e^{j\omega_0 T_s n} \\ &= \left(1 + \sum_{l=-\infty}^{\infty} \Lambda(\omega_0, l)\right) e^{j\omega_0 T_s n} \\ &= \frac{1}{1 + P_d(j\omega_0)C[e^{j\omega_0 T_s}]} e^{j\omega_0 T_s n} \\ &= S_d(j\omega_0)e^{j\omega_0 T_s n}, \end{aligned} \quad (15)$$

where $S_d(j\omega_0)$ is the sensitivity function at ω_0 in a discrete-time system.

Equation (15) indicates that when $\sum_{l=-\infty,\neq 0}^{\infty} |\Lambda(\omega_0, l)|$ is sufficiently small, S_{sd} can be given by

$$S_{sd}(j\omega_0) \simeq S_d(j\omega_0). \quad (16)$$

Therefore, the control system can suppress the vibration, in which the frequency is ω_0 when

$$|W(j\omega_0)P_c(j\omega_0)| \gg \sum_{l=-\infty,\neq 0}^{\infty} |W(j\omega_0 + j\omega_s l)P_c(j\omega_0 + j\omega_s l)| \quad (17)$$

$$|S_d(j\omega_0)| < 1 \quad (18)$$

4. DISTURBANCE SUPPRESSION USING MULTI-RATE RESONANT FILTER

To suppress the disturbance beyond the servo bandwidth of the control system, the control system should have stable resonant characteristics at the disturbance frequency [Atsumi et al. (2005, 2007)]. However, (17) indicates that the control system should have small gains at aliasing frequencies of the disturbance frequency. Therefore, when the disturbance frequency is higher than the Nyquist frequency, the control system should realize the resonant characteristics by using continuous-time filters or multi-rate filters. In this paper, a design method that uses the multi-rate filter is proposed.

The multi-rate filter F_m is given by the following equation:

$$F_m[z] = 1 + F_r[z], \quad (19)$$

where F_r is the multi-rate resonant filter. When $F_r[z] = 0$, the transfer characteristics from u_d to y_d at ω_0 are given by follows:

$$P_{d0}(j\omega_0) = \frac{1}{T_s}\sum_{k=-\infty}^{\infty} W_0(j\omega_0 + j\omega_s k)P_c(j\omega_0 + j\omega_s k), \quad (20)$$

where

$$W_0(j\omega) = I_p[e^{j\omega T_s/m}]\mathcal{H}_m(j\omega). \quad (21)$$

Here, the disturbance frequency is defined as ω_r. To suppress the disturbance, F_r should have stable resonant characteristics at ω_r, and the control system, which includes F_r, should satisfy the following equation [Atsumi et al. (2007)]:

$$\angle\left[P_d(j\omega_r)C[e^{j\omega_r T_s}]\right] = \arctan\left(\frac{b_r(\omega_r)}{a_r(\omega_r) + 1}\right), \quad (22)$$

where

$$a_r(\omega_r) = \mathrm{Re}\left[P_{d0}(j\omega_r)C[e^{j\omega_r T_s}]\right], \quad (23)$$

and

$$b_r(\omega_r) = \mathrm{Im}\left[P_{d0}(j\omega_r)C[e^{j\omega_r T_s}]\right]. \quad (24)$$

5. CONTROL SYSTEM DESIGN

The sampling time T_s of the hard disk drive used in this study was 76.7 μs ($\omega_s = 2\pi \times 13000$ [rad/s] and the Nyquist frequency was 6500 Hz). The frequency of disturbance ω_r is set to 7000 Hz. The frequency response of the mechanical system is indicated by the dashed line in Fig. 3.

5.1 Controlled object

It is assumed that $|P_c(j\omega)|$ is vanishingly small when $\omega > 2\omega_s$. Thus, to reduce the calculation load, the frequency response of $P_c(j\omega)$ is defined as

$$P_c(j\omega) = \begin{cases} P_{c0}(j\omega) : |\omega| \le 2\omega_s, \\ 0 : |\omega| > 2\omega_s. \end{cases} \quad (25)$$

P_{c0} is assumed to be given by the product of the "mechanical model P_s" and the "equivalent dead-time model P_{dl}."

$$P_{c0}(s) = P_s(s) \cdot P_{dl}(s). \quad (26)$$

Table 1. Parameters of $P_s(s)$

l	$\omega_{nk}(l)$	$\alpha_k(l)$	$\zeta_k(l)$
1	0	1.00	0
2	$2\pi \cdot 4100$	−1.30	0.01
3	$2\pi \cdot 5700$	−0.03	0.01
4	$2\pi \cdot 6200$	−0.08	0.01
5	$2\pi \cdot 7650$	0.12	0.02
6	$2\pi \cdot 8900$	−0.13	0.02
7	$2\pi \cdot 9800$	−0.35	0.03

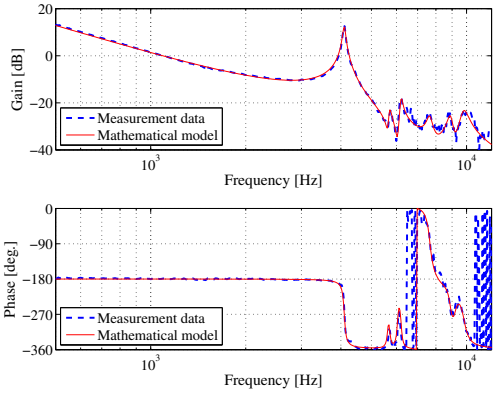

Fig. 3. Frequency response of mechanical system

The mechanical model P_s is given by follows [Atsumi et al. (2003)]:

$$P_s(s) = K_p \sum_{l=1}^{\psi} \frac{\alpha_k(l)}{s^2 + 2\zeta_k(l)\omega_{nk}(l)s + \omega_{nk}(l)^2}, \qquad (27)$$

where ψ is the number of modes, α_k is the residue of each mode, ω_{nk} and ζ_k are the natural frequency [rad/s] and the damping ratio of the resonance, respectively, and K_p is the plant gain. These parameters were fixed so that the model's frequency response coincided with the measured result indicated by the dashed line in Fig. 3. To be more precise, ψ was set to seven (the model order is fourteen), K_p to 4.3×10^7, and the values of the other parameters are listed in Table 1. The solid line in Fig. 3 represents the frequency response of this mathematical model.

The equivalent dead-time model P_{dl}, which includes the characteristics of the dead-time element, is given by follows [Franklin et al. (1980)]:

$$P_{dl}(s) = e^{-\tau s}, \qquad (28)$$

where τ is the equivalent dead time. Here, τ of the hard disk drive used in this study is 10 μs.

5.2 Multi-rate hold and interpolator

In this paper, the multi-rate number m is set to two. The multi-rate hold $\mathcal{H}_m$ is a zero-order hold (ZOH) and the transfer characteristic is given by the following equation:

$$\mathcal{H}_m(s) = \frac{1 - e^{-(T_s/2)s}}{s}. \qquad (29)$$

The interpolator consists of an up-sampler and an interpolation filter. The transfer function of the interpolation filter can be given by

$$I_p[z] = 1 + z^{-1}. \qquad (30)$$

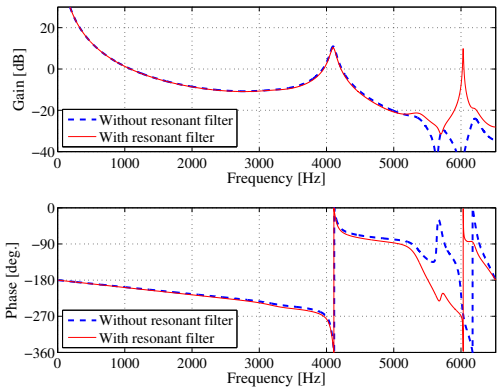

Fig. 4. Frequency response of controlled object

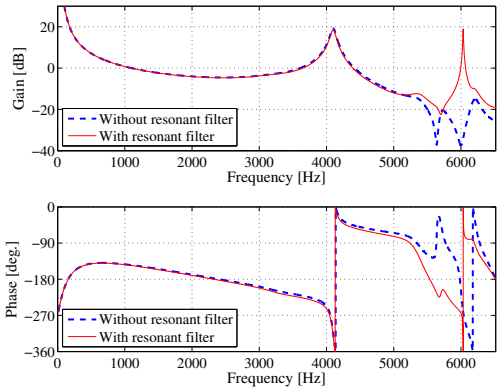

Fig. 5. Frequency response of open-loop characteristics

5.3 Controller design

First, the single-rate controller $C[z]$, which stabilizes the control system, is given by the "PI-lead filter" and designed for the controlled object P_{d0} in which $F_m[z] = 0$. The frequency response of P_{d0} is indicated by the dashed line shown in Fig. 4. To make the phase margin more than 30°, the gain margin more than 4.5 dB, and the open-loop gain 0-dB crossover frequency 1100 Hz, C is set according to the following equation:

$$C[z] = \frac{11.8(z - 0.908)(z - 0.953)}{(z - 0.161)(z - 1)}. \qquad (31)$$

The frequency response of $P_{d0}C$ (the open-loop characteristics without the resonant filter) is indicated by the dashed line in Fig. 5.

To suppress the disturbance, F_m should have stable resonant characteristics at ω_r. From (22) and $\omega_s/2 < \omega_r < \omega_s$, the phase of the multi-rate resonant filter at the disturbance frequency ω_r should be

$$\begin{aligned} &\angle F_{m0}[e^{j\omega_r T_s/2}] = -\angle P_c(j\omega_r) - \angle I_p[e^{j\omega_r T_s/2}] \\ &-\angle H_m(j\omega_r) - \angle C[e^{j\omega_r T_s}] - \arctan\left(\frac{b_r(\omega_r)}{a_r(\omega_r) + 1}\right), \end{aligned} \qquad (32)$$

where

$$F_{m0}[z] = F_m[z] - 1. \qquad (33)$$

As a result, $F_m[z]$ was set as follows:

$$F_m[z] = 1 + \frac{0.0479(z - 4.37)(z - 1)}{(z^2 + 0.233z + 0.998)}. \qquad (34)$$

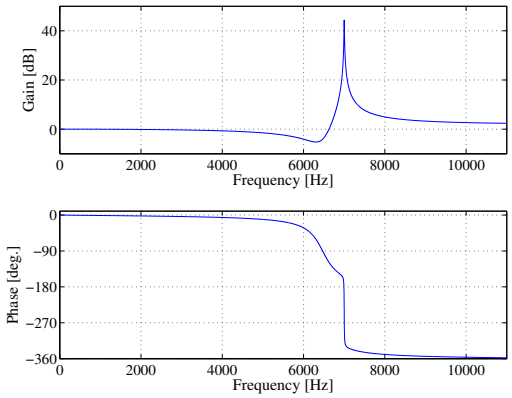

Fig. 6. Frequency response of F_m

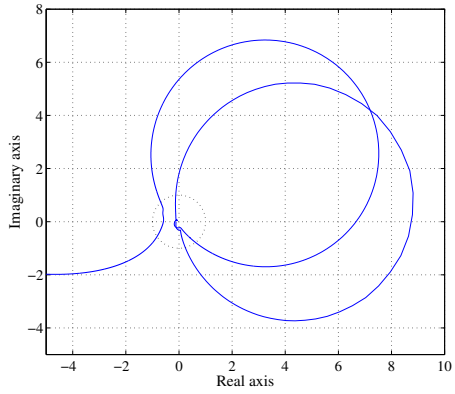

Fig. 7. Nyquist diagram

The frequency response of F_m is shown in Fig. 6, and the frequency response of P_d is indicated by the solid line in Fig. 4.

The characteristics of the control system with the resonant filter are indicated as follows. The frequency response of the open-loop characteristics is indicated by the solid line in Fig. 5. The Nyquist diagram is indicated in Fig. 7, and the gain of the sensitivity function in discrete-time system S_d is indicated in Fig. 8. These figures indicate that (18) is satisfied by using the resonant filter, and (17) is also satisfied because

$$|W(j\omega_r)P_c(j\omega_r)| = 3.11, \tag{35}$$

and

$$\sum_{l=-\infty,\neq 0}^{\infty} |W(j\omega_r + j\omega_s l)P_c(j\omega_r + j\omega_s l)| = 0.11. \tag{36}$$

By using the design results of the control system and (14), the gain-frequency responses of the sensitivity functions in sampled-data control systems were calculated. The frequency responses of $|P_{sd}|$ are shown in Fig. 9. As indicated by this figure, the control system suppresses the disturbance at 7000 Hz.

6. SIMULATION AND EXPERIMENT

The simulation results of Fig. 2, in which the frequency of disturbance signal d_c is 7000 Hz, and the vibrational amplitude is 0.1 track, are calculated. In Fig. 10, the dashed line represents the signal of y_c without the resonant

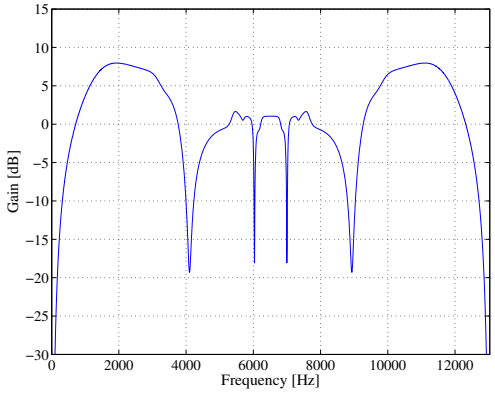

Fig. 8. Frequency response of $|S_d|$

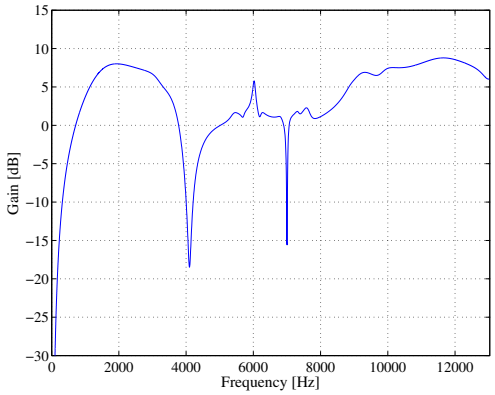

Fig. 9. Frequency response of $|S_{sd}|$

filter, and the solid line represents the signal of y_c with the resonant filter. In Fig. 11, the dashed line represents the signal of y_d without the resonant filter, and the solid line represents the signal of y_d with the resonant filter. These figures indicate that the control system decreases vibrations in which the frequency is higher than the Nyquist frequency.

To show the effect of the proposed method, we did an experiment using the conditions similar to those of the simulation. In these experiments, the sampling time of y_c is 38.4 μs (1/2 of T_s) because the continuous-time signal cannot be measured in actual head-positioning systems. The time response of y_c is shown in Fig. 12, and the time response of y_d is shown in Fig. 13. In both figures, the dashed line represents the results without the resonant filter, and the solid line represents the results with the resonant filter. These experimental results also indicate that the control system decreases vibrations whose frequency is higher than the Nyquist frequency. The differences between the simulation result and the experimental result are caused by disturbances other than the disturbance signal d_c in the actual head-positioning system.

7. CONCLUSION

A control system design method that suppresses disturbances beyond the Nyquist frequency was proposed. This method uses frequency responses of a controlled object and digital controller for calculations of the gain of the sensitivity function in a sampled-data system without complex calculations involving matrices, and realizes a stable

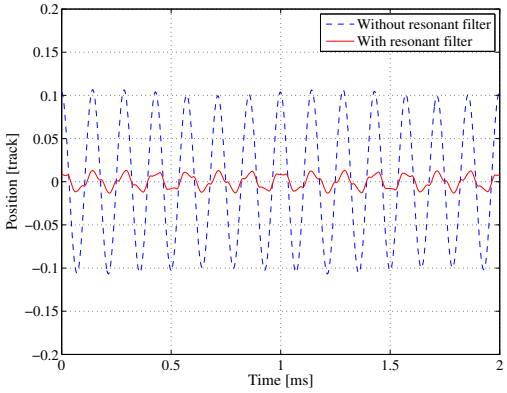

Fig. 10. Simulation results of y_c

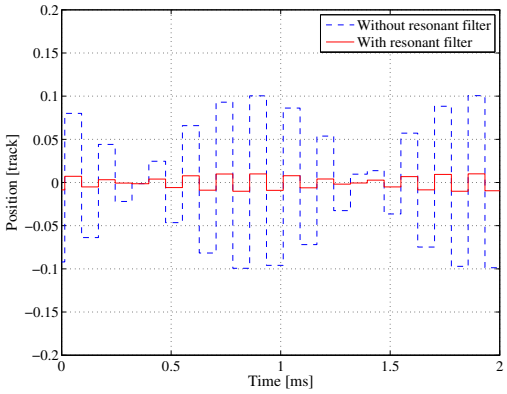

Fig. 11. Simulation results of y_d

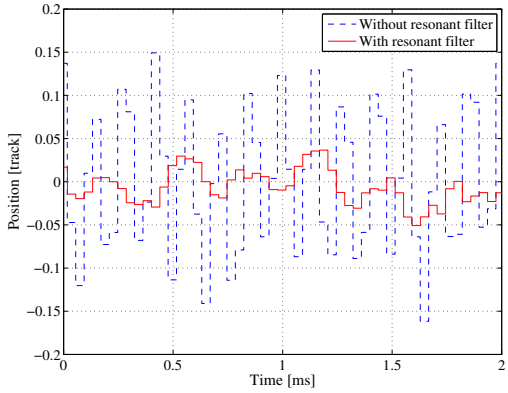

Fig. 12. Experimental results of y_c

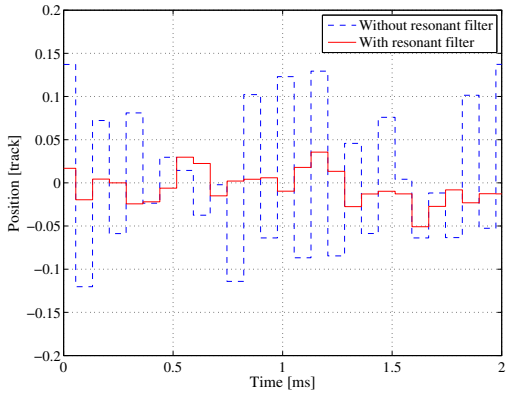

Fig. 13. Experimental results of y_d

resonant filter that decreases the gain of the sensitivity function above the Nyquist frequency. When the method was applied to the head-positioning system of a hard disk drive, the experimental results indicated that the control system suppresses the disturbance in which the frequency was higher than the Nyquist frequency.

REFERENCES

P. Lyman, H. R. Varian, K. Swearingen, P. Charles, N. Good, L. L. Jordan and J. Pal. How Much Information? 2003. The School of Information Management and Systems at the University of California at Berkeley, 2003.

T. Atsumi, T. Arisaka, T. Shimizu, and T. Yamaguchi. Vibration Servo Control Design for Mechanical Resonant Modes of a Hard-Disk-Drive Actuator. *JSME International Journal Series C*, volume 46, number 3, pages 819–827, 2003.

T. Atsumi, T. Arisaka, T. Shimizu, and H. Masuda. Head-Positioning Control Using Resonant Modes in Hard Disk Drives. *IEEE/ASME Transactions on Mechatronics*, volume 10, number 4, pages 378–384, 2005.

P. A. Weaver and R. M. Ehrlich. The Use of Multirate Notch Filters in Embedded-Servo Disk Drives. *Proceedings of the American Control Conference,* volume 6, pages 4156–4160, 1995.

M. Hirata, T. Atsumi, A. Murase, and K. Nonami. Following Control of a Hard Disk Drive by using Sampled-Data H_∞ Control. *The 1999 IEEE International Conference on Control Applications*, Kohala Coast-Island of Hawaii, Hawaii, pages 182–186, 1999.

Y. Gu and M. Tomizuka. Digital Redesign and Multirate Control for Motion Control -a general approach and application to hard disk drive servo system. *Proceedings of The 6th IEEE International Workshop on Advanced Motion Control,* pages 246–251, 2000.

T. Semba. An H_∞ Design Method for a Multi-Rate Servo Controller and Applications to a High Density Hard Disk Drive. *Proceedings of the 40th IEEE Conference on Decision and Control,* pages 4693–4698, 2001.

T. Hara. Openloop Gain Criteria of Sampled-data Control Systems with Mechanical Resonant modes above the Nyquist Frequency. *Proceedings of The SICE-ICASE International Joint Conference 2006*, pages 2771-2776, 2006.

G. F. Franklin and J. D. Powell. *Digital Control of Dynamic Systems.* Addison and Wesley, Menlo Park, California, 1980.

S. Hara, H. Fujioka, P. P. Khargonekar and Y. Yamamoto. Computational Aspects of Gain-Frequency Response for Sampled-Data Systems. *Proceedings of the 34th Conference on Decision and Control,* pages 1784–1789, 1995.

Y. Yamamoto and P. Khargonekar. Frequency response of sampled-data systems. *IEEE Transactions on Automatic Control,* volume 39, pages 166–76, 1996.

T. Atsumi, A. Okuyama, and M. Kobayashi. Track-following Control Using Resonant Filter in Hard Disk Drives. *The 2007 American Control Conference* pages 61–67, 2007.